

Structure of Random Porous Materials: Silica Aerogel

Dale W. Schaefer and Keith D. Keefer

Sandia National Laboratories, Albuquerque, New Mexico 87185

(Received 25 March 1985; revised manuscript received 11 March 1986)

Using small-angle x-ray scattering, we show that porous silica aerogel has a fractal backbone structure. The observed structure is traced to the underlying chemical (polymerization) and physical (colloid aggregation) growth processes. Comparison of scattering curves for aerogel with silica aggregates confirms this interpretation.

PACS numbers: 68.70.+w, 61.10.Lx, 82.70.Dd, 82.70.Rr

In spite of the importance of random porous media in nature and in technology, the structure of these materials has eluded characterization. In this paper we show that certain classes of porous materials can be characterized through fractal geometry and that the appropriate geometry can be determined by small-angle x-ray scattering. We report the structure of a silica aerogel prepared by critical-point drying of an alcoholic (sic) silica gel. This material is chosen because of its exceedingly low density (0.09 g/cm^3) and concomitant high porosity. We show that the porosity in this material is due to a random colloid aggregation process in the solution precursor. To our knowledge, this is the first time that the structure of a porous material has been explained in terms of random growth.

Classical models of porosity-dependent properties are based on highly simplified geometrical structures like packed spheres or bottlenecked bubbles.¹ Recently, fractal² structures (percolation networks, fractal surfaces) have also been postulated to explain fluorescence³ and adsorption^{4,5} data for porous media. Although there have been many attempts to characterize the microstructure of porous materials, model-dependent geometric assumptions, like those above, have doomed all indirect methods.

A primary goal of our work is to establish the existence of a fractally porous solid. To this end, we first outline the expected scattering patterns for simple fractal structures. The key to our interpretation is based on a qualitative distinction between surface and volume fractals. We find that the low-density aerogel has purely mass-fractal character and find no evidence for fractally rough surfaces.

Scattering from fractals.—To interpret scattering curves it is useful to distinguish between bulk and surface scattering. In systems without distinct surfaces, such as polymers in solutions, the scattered intensity, I , often obeys a power law in the magnitude of the scattering vector, K (at a given scattering angle one probes fluctuations of Fourier spatial frequency K),

$$I(K) \sim K^{-D}, \quad (1)$$

where D is the fractal dimension relating mass, M , to length, R . If one imagines measuring the mass within

a sphere of radius R , then,

$$M(R) \sim R^D. \quad (2)$$

Note that for rods, disks, and spheres, D is 1, 2, and 3, respectively, consistent with the common notion of dimensionality. For random objects, however, D may be noninteger and thus D is known as the fractional or fractal dimension.² We call the regime where Eq. (1) applies the Porod region of the scattering curve.

Objects obeying Eq. (2) are called mass or volume fractals. Examples include polymers,⁶ diffusion-limited aggregates,⁷ and percolation clusters.⁸ Scattering from mass fractals is discussed in detail by Schaefer and Keefer.⁹

Note that Eq. (1) applies only in the regime $\xi \gg K^{-1} \gg a$, where ξ is the correlation range and a is a typical chemical or bond distance. For distances large compared to ξ (i.e., $K^{-1} \gg \xi$) the object is likely to be uniform and $I(K)$ is independent of K . For $K^{-1} \sim a$ one probes atomic distances and scattering curves reflect local short-range order. For solid objects with mass fractal character, ξ can usually be identified with the mean pore size. This identification follows because pores are always correlated over length scales that are comparable to their radius. In this paper we are concerned with the intermediate or Porod regime, $\xi \gg K^{-1} \gg a$, where Eq. (1) is valid and where scattering probes the scale-independent properties of the system.⁹

Equation (1) contrasts with that for surface fractals.^{4,5} These objects are uniform, so that no scattering occurs from the bulk, only from the surface. For this case, Bale and Schmidt¹⁰ have shown

$$I(K) \sim K^{D_s-6}, \quad (3)$$

where D_s is the surface fractal dimension which relates surface area, S , to length. If one measures the surface within a sphere of radius R , then,

$$S \sim R^{D_s}. \quad (4)$$

Fractal surfaces are rough on all length scales up to some surface correlation range ξ_s , beyond which they are smooth. A crossover to smooth surfaces may also occur at small length scales.

Several aspects of surface scattering should be noted. First, for smooth surfaces $D_s = 2$ and the scattered intensity decays as K^{-4} in Eq. (3). This behavior is commonly called Porod's law, and so Eq. (3) is a generalization of Porod's law. For fractal surfaces ($2 < D_s < 3$) Porod slopes between -3 and -4 are expected. Solid objects with fractally rough pores may display very complex scattering curves with crossovers between uniform, smooth, and fractally rough regimes. Clearly, interpretation of such a system would be difficult.

The above discussion shows that the two classes of fractal objects can be distinguished according to the observed slope of the scattering curve in the Porod regime. Mass fractals have slopes between -1 and -3 . Surface fractals have slopes between -3 and -4 . Cognizance of these categories is essential to interpretation of the scattering from porous aerogel.

Experiment.—The silica aerogel used in these experiments was obtained from Airglass AB, Sjöbo, Sweden. The material is prepared by base-catalyzed hydrolysis and condensation of silicon tetramethoxide (TMOS) in alcohol.¹¹ The condensation ultimately leads to a gel which is critical-point dried to remove the solvent. The resulting porous solid is nearly transparent. The material used in these experiments has a density of $8.8 \times 10^{-2} \text{ g/cm}^3$.

Data are also reported for water suspension of stabilized and of aggregated colloidal silica. In the case of the suspension (Ludox SM) the system was studied at high dilution (0.1 wt.%) to avoid complication of the scattering curves due to electrostatic interactions. The aggregates were studied at 0.5 wt.% and were prepared¹² by a decrease of the pH to 5.5 and an increase of the ionic strength of the solution to 0.5M with NaCl.

The small-angle x-ray scattering (SAXS) measurements were made with an Anton-Paar compact Kratky camera which had been modified to mount on a Rigaku RU200 12-kW rotating anode x-ray generator and to use a TEC model 205 position-sensitive proportional counter. Copper $K\alpha$ ($\lambda = 1.542 \text{ \AA}$) radiation was selected with a graphite monochromator. The sample to detector distance was 211 mm. With operation at $< 40 \text{ kV}$ and 20 mA , the curves shown in Fig. 1 were obtained in 500–1000 sec. The data were not corrected for either detector linearity or sensitivity. At the present stage of development, such corrections are smaller than our ability to measure them. A solvent background, however, was subtracted for the solution samples. Both the aggregation and the SAXS experiments were performed at room temperature, $(24 \pm 3)^\circ\text{C}$. Because of the line geometry of the Kratky system the data were desmeared to allow comparison with calculated exponents. In the case of aerogel and stabilized colloidal silica, desmearing was ac-

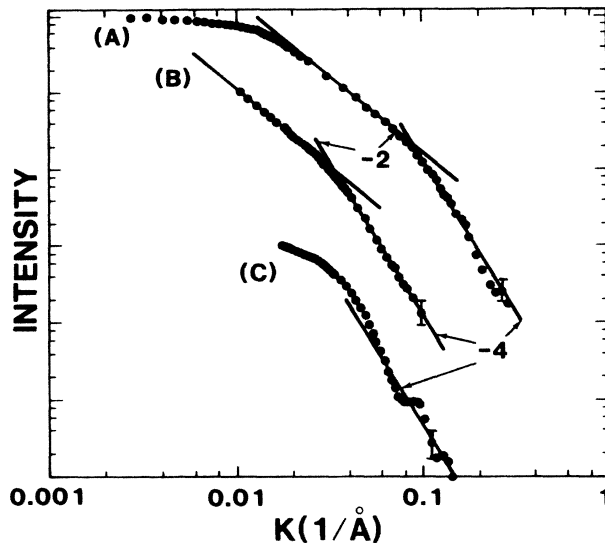


FIG. 1. Small-angle x-ray scattering curves for (curve A) silica aerogel ($\rho = 0.088 \text{ g/cm}^3$), (curve B) a solution aggregate of silica particles (Ref. 12), and (curve C) the colloidal monomer. No crossover to K independence at small K is observed for the aggregate because of the large size ($> 1 \mu\text{m}$). The similarity of curves A and B indicates that the aerogel and the aggregate are structurally similar. More extensive light scattering data (Ref. 13) show a slope of -2.1 for the aggregate in the regime $K < 0.01 \text{ \AA}^{-1}$.

complished by use of Glatter's procedure.¹⁴ For the aggregates, however, this procedure failed because of the lack of a maximum length scale. The aggregate data were analytically desmeared by a division of the observed intensity by K . This procedure is exact in power-law regimes but is questionable in crossover regimes.

Results.—The scattering curve for silica aerogel is shown as the top curve of Fig. 1. Three distinct regimes are apparent. At small K the data are K independent, consistent with a uniform, nonfractal long-range structure. The correlation range, ξ , was obtained from the crossover in the low- K portion of the curve, with the result $\xi = 90 \text{ \AA}$.

For $K > 0.01$, two power-law regimes are seen with slopes of -2 and -4 , consistent with Eqs. (1) and (3) with $D = 2$ and $D_s = 2$, respectively. The crossover occurs at $K = 0.09 \text{ \AA}^{-1}$, corresponding to a length $b \equiv K^{-1} = 11 \text{ \AA}$. The picture that emerges then is scattering from a smooth surface at short length scales ($< b$) and scattering from a mass fractal of dimension 2 at larger scales. For lengths larger than ξ the structure is uniform suggesting that this is the mean radius of the pores and the upper limit of the fractal structure.

The most reasonable structure consistent with the data is shown schematically in Fig. 2. Basically the porosity is due to a random "jungle gym" or

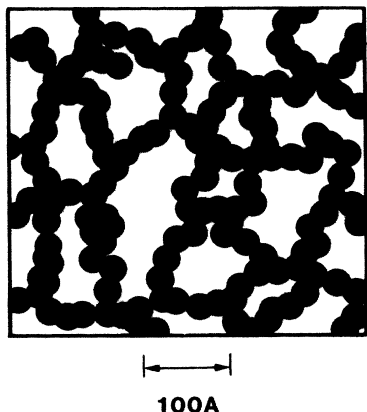


FIG. 2. Schematic diagram of the structure suggested for silica aerogel.

branched-polymer-like structure. The network backbone is characterized by the radius b and is smooth on scales shorter than b . For intermediate length scales ($> b$, $< \xi$), the structure is chainlike and looks like a randomly branched polymer made up of "monomers" of radius b . For length scales beyond ξ the structure is uniform. Although the detailed structure of the backbone cannot be inferred from the data, the structure indicated in Fig. 2 is consistent with the colloidal model suggested below for the origin of the structure.

Discussion.—In principle, analytic expressions could be developed for the entire scattering curve. Simplified expressions, for example, were used to study silica¹⁵ and TiH_2 aggregates.¹⁶ In our opinion, however, the functions used lead incorrectly to the conclusion that fractal structures had been observed. The problem is that the functions near the crossover are not known except for linear polymers¹⁷ and the proliferation of parameters dilutes the data analysis. We choose to deal with this issue (see below) by comparing the data to a model (a known colloidal aggregate). In addition, we show that the observed scattering curve is distinctly different from a nonfractal system (the stabilized colloid). We believe that the structure of porous aerogel is identical to a colloidal aggregate grown in the solution precursor. This explanation is not only consistent with the observed scattering but it is also consistent with the chemical conditions in the precursor. During polymerization^{18,19} silica particles grow to a mean radius b and then aggregate in a ramified manner and ultimately gel.

To test the colloid-aggregation idea, we studied the growth of silica aggregates in a separate experiment.¹² These data are shown in curve *B* of Fig. 1. These data were taken after large aggregates had formed. No Guinier regime^{9,20} is observed, which is consistent with the formation of large clusters which never gel because of the very low concentration. The similarity of the curves is striking, including the observed slopes

of -2 and -4 with a very sharp crossover. The similarity confirms that colloid aggregation is the controlling growth process which determines the structure of the porous solid. It is the similarity of the curves not the exact slope which is important to this conclusion. Light scattering¹³ shows the asymptotic slope of the aggregate data to be -2.1 for $K < 0.01 \text{ \AA}^{-1}$. The difference (5%) represents a reasonable error introduced by the limited power-law regime in the aerogel data. Errors in this range are consistent with the analysis of Teixeira²¹ when ξ/b is between 5 and 10.

It should be noted that the aerogel and aggregate scattering curves are distinctly different from that of the colloidal monomer shown in curve *C* of Fig. 1. In this case, the system has only one length scale (the particle radius, R) and no power-law regime is found near $K = 0.01 \text{ \AA}^{-1}$. At large K , this curve falls off as a smoothed Bessel function, characteristic of a nearly monodisperse collection of noninteracting spherical particles.²¹ Scattering from such a system is expected to display a minimum near $4.5/R$ consistent with the data.

The structure inferred here is also consistent with the ideas of Iler,¹⁹ who suggests that *aqueous silica gelation* proceeds by growth (polymerization of silicic acid) and aggregation of colloidal particles. Although noncolloidal silicate polymers are known,²² we believe that colloidal particles are produced for TMOS hydrolyzed under alkaline conditions with excess water. Under these conditions the polymerizing species is probably silicic acid,¹⁸ the same species which is known to polymerize to dense particles in aqueous systems.¹⁹

Since our interpretation is not unique, we considered the classic model of random sharp interfaces proposed by Debye, Anderson, and Brumberger.²³ This model yields a squared-Lorentzian profile, which fits the data very poorly. Functions with more variables can be generated which do fit the data. Since we have neither a chemical nor physical basis for such analysis, however, we consider the interpretation given above to be superior.

As suggested earlier, caution must be exercised in the interpretation of curves with more than one power-law regime. The model presented here is not only consistent with the data (i.e., the similarity of the curves in Fig. 1) it also is consistent with our previous work on silica chemistry. These factors, coupled with the lack of a consistent competing structure, make us confident of the interpretation given.

The novel structure found for silica aerogel shows that care must be taken when porous materials are used as models for dynamics in random media. The common notion of packed spheres or connected bubbles is not seen in this aerogel. Clearly, other fractal-dependent properties such as diffusion in fractals (as

well as absorption of gases) depend on exactly what type of structure is present. Also, our material, which is extremely low density, displays fractal character only over one decade in length scale. This result suggests that fractal character found^{3,4} for other less-porous materials is probably not related to structure at all. Finally, note that it is the backbone, not the pore space, which is fractal.

Our analysis suggests that the structure of colloid-derived porous materials can be modified through the aggregation process itself. In particular, since multiparticle diffusion-limited aggregation²⁴ gives a lower fractal dimension (1.8 versus the observed 2.0), a lower-density material could be produced by more aggressive aggregation conditions. Moreover, novel porous structures derived from either polymers¹⁸ or fractally rough colloids²⁵ are possible.

We thank B. C. Bunker for bringing the aerogel material to our attention and for cutting the sample. We thank R. J. Birgeneau for suggesting the alternative method of data analysis. We thank D. P. Evans for technical assistance. This work was performed at Sandia National Laboratories and was supported by the U. S. Department of Energy under Contract No. DE-AC04-76DP00789.

¹S. J. Gregg and K. S. W. Sing, *Adsorption, Surface Area and Porosity* (Academic, London, 1982).

²B. B. Mandelbrot, *Fractals, Form and Chance* (Freeman, San Francisco, 1977).

³U. Even, K. Rademann, J. Jortner, N. Manor, and R. Reisfeld, *Phys. Rev. Lett.* **52**, 2164 (1984).

⁴D. Avnir, D. Farin, and P. Pfeifer, *Nature* **308**, 5956 (1984).

⁵P. Pfeifer and D. Avnir, *J. Chem. Phys.* **79**, 3558, 3566 (1983).

⁶D. W. Schaefer and J. G. Curro, *Ferroelectrics* **30**, 49 (1980).

⁷T. A. Witten and L. M. Sander, *Phys. Rev. Lett.* **47**, 1400 (1981).

⁸D. Stauffer, *Introduction to Percolation Theory* (Taylor and Francis, Philadelphia, 1985).

⁹D. W. Schaefer and K. D. Keefer, *Mat. Res. Soc. Symp. Proc.* **32**, 1 (1984).

¹⁰H. D. Bale and P. W. Schmidt, *Phys. Rev. Lett.* **53**, 596 (1984).

¹¹S. Henning and L. Svensson, *Phys. Scr.* **23**, 697 (1981).

¹²D. W. Schaefer, K. D. Keefer, and J. E. Martin, *J. Phys. (Paris), Colloq.* **46**, C3-127 (1985).

¹³D. W. Schaefer, J. E. Martin, P. Wiltzius, and D. S. Cannell, *Phys. Rev. Lett.* **52**, 2371 (1984).

¹⁴O. Glatter, *J. Appl. Cryst.* **13**, 7 (1980).

¹⁵S. K. Sinha, T. Freltoft, and J. Kjems, in *Kinetics of Aggregation and Gelation*, edited by F. Family and D. P. Landau (North-Holland, Amsterdam, 1984), p. 87.

¹⁶Ph. Mangin, B. Rodmacy, and A. Chamberod, *Phys. Rev. Lett.* **55**, 2899 (1985).

¹⁷J. E. Martin and B. J. Ackerson, *Phys. Rev. A* **31**, 1180 (1985).

¹⁸K. D. Keefer, *Mat. Res. Soc. Symp. Proc.* **32**, 15 (1984).

¹⁹R. K. Iler, *The Chemistry of Silica* (Wiley, New York, 1979).

²⁰H. B. Stuhmann and A. Miller, *J. Appl. Cryst.* **11**, 325 (1978).

²¹J. Teixeira, in *On Growth and Form*, edited by H. E. Stanley and N. Ostrowsky (Martinus Nijhoff, Boston, 1985), p. 145.

²²D. W. Schaefer and K. D. Keefer, *Phys. Rev. Lett.* **53**, 1383 (1984).

²³P. Debye, H. R. Anderson, and H. Brumberger, *J. Appl. Phys.* **28**, 679 (1957).

²⁴P. Meakin, *Phys. Rev. Lett.* **51**, 1119 (1983).

²⁵K. D. Keefer and D. W. Schaefer, to be published.